STM-induced luminescence study of poly(*p*-phenylenevinylene) by conversion under ultraclean conditions

Santos F. Alvarado,* Walter Rieß, and Paul F. Seidler
IBM Research Division, Zurich Research Laboratory, 8803 Rüschlikon, Switzerland

Peter Strohriegl
University of Bayreuth, Makromolekulare Chemie I and BIMF, 95440 Bayreuth, Germany
(Received 14 November 1996)

Curing-temperature-dependent spectroscopic studies of the conversion process of the sulfonium chloride prepolymer to the conjugated polymer poly(*p*-phenylenevinylene) reveal an enhancement of the luminescence efficiency when the films are converted under ultrahigh-vacuum conditions. In these experiments, luminescence is excited by electron injection from the tip of a scanning tunneling microscope and the maximum luminescence efficiency is found between 225 °C and 260 °C. The optimum conversion temperature, the total luminescence yield, and the spectral features of the luminescence depend on the substrate material, heating gradient, and composition and purity of the prepolymer. The curing-temperature dependence of the Franck-Condon intensity distribution has a complex behavior. Maximum luminescence efficiency is characterized by a spectrum where the $v=0,1$ vibronic transition has maximum relative intensity. Images of scanning-tunneling-microscopy-excited luminescence show intensity fluctuations within surface domains as small as a few nanometers in diameter, regions that correlate with the topographic features of the poly(*p*-phenylenevinylene) surface. [S0163-1829(97)02028-6]

I. INTRODUCTION

Organic light-emitting diodes (OLED's) have become attractive candidates for the realization of low-cost, flat, lightweight, and even flexible displays.[1] Among the various classes of light-emitting organic materials used in these devices, semiconducting, conjugated polymers in particular are engendering a great deal of interest because of their ease of processability.[2,3] The observation of electroluminescence (EL) from poly(*p*-phenylenevinylene) (PPV) has provided much of the impetus for this field, and the family of light-emitting polymers based on PPV continues to be the focus of many studies to improve device efficiency and prolong lifetime.[4,5]

In the fabrication of OLED's based on PPV itself, the PPV film is formed via a precursor route, the last step of which typically involves thermal treatment of a sulfonium chloride prepolymer. Because of the complex chemistry and physics involved, the details of this conversion procedure are critical,[6] determining the photoluminescence (PL) efficiency and influencing charge injection and transport.[2,6–9] Wide variations of the electrical conductivity, PL and EL yield, as well as the spectroscopic signature of the end product are found even for samples produced within the same laboratory.

In order to elucidate the influence of curing temperature, substrate, heating gradient, and other environmental factors on PPV film preparation, we performed a spectroscopic study of the prepolymer conversion process using scanning tunneling luminescence (STL). With this method, light emission from the polymer is excited by injecting charge carriers from the tip of a scanning tunneling microscope (STM).[10] The possibility of using a STM to excite light emission with nanometer resolution and to probe the electronic properties of device structures has been demonstrated in experiments on III-V quantum wells[11,12] and quantum wires.[13] In the work described here, the STL technique simulates the operation of an OLED, but in a very localized fashion. By exciting EL without the cathode having to be in physical contact with the polymer, STL also separates the behavior of the organic layer from the physical and chemical properties of the cathode and cathode interface. This is useful for understanding injection processes as well as cathode-induced degradation effects. Combined with the fact that we carry out the thermal conversion of our films in ultrahigh vacuum (UHV), we are able to monitor precursor conversion under highly controlled conditions. We find strong evidence of a correlation between luminescence efficiency and spectroscopic features, such as the Franck-Condon intensity distribution of the vibronic lines, and the homogeneity and ordering of the polymer chains.

II. EXPERIMENTAL METHODS

Three types of STL experiments were performed: (i) spatially resolved image collection, where total light emission is observed while scanning the STM tip across the sample; (ii) measurement of wavelength-integrated luminescence intensity at a given point on the sample for the determination of luminescence efficiency; and (iii) STM-excited luminescence spectroscopy, in which an energy-resolved emission spectrum is recorded at a given point on the sample. The latter is illustrated schematically in Fig. 1. The STM and optics for collecting the emitted light are mounted in an UHV chamber (base pressure in the lower 10^{-10}-mbar range), luminescence is observed from the free surface of the film, and the complete optical system is adjustable in the x, y, and z directions to allow optimum alignment. Outside the chamber, an optical fiber transmits the collected light to an optical multichannel

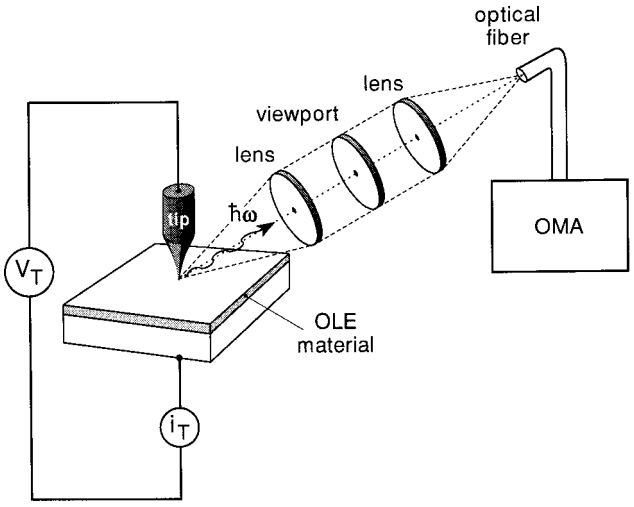

FIG. 1. Experimental setup used for the STM-based luminescence excitation. For the measurement of the wavelength-integrated intensity, e.g., for luminescence maps, the optical fiber and the optical multichannel analyzer (OMA) are replaced by an avalanche photodiode.

analyzer (OMA). For spatially resolved image collection and measurements of wavelength-integrated luminescence intensity, the OMA and optical fiber are replaced by an avalanche photodiode. A load lock (base pressure in the 10^{-7}-mbar range) is attached to the UHV system to allow insertion of STM tips and samples and both the load lock and the UHV chamber have a heating stage for thermal treatment of the samples. Commercially available PtIr tips as well as electrochemically etched W tips were used.

The sulfonium chloride prepolymer poly(*p*-phenylene-ethylene-tetrahydrothiophenium chloride) was synthesized by a modification[14] of the Wessling route. Films were prepared by coating a methanol-acetone solution of the prepolymer onto (indium thin oxide) ITO-on-sapphire or Au-on-glass substrates using the doctor-blade technique and allowing the solvent to evaporate under ambient conditions. The nominal thickness of the prepolymer films ranged between 180 and 200 nm. Coated substrates were then cut into approximately 6×6 mm^2 squares, which were placed in the load lock within about 1 h of the coating process.

STL characterization of the polymer films was performed at room temperature after heating a given sample to progressively higher curing temperatures T_c in the UHV chamber. Curing times varied with temperature, and typical values were up to 1 day for the range 140 °C–160 °C, 12 h at 240 °C, and 2–2.5 h for $T_c>325$ °C. In some cases we checked to ensure that prolonging the curing time did not change the spectra significantly. For comparison, films were also cured in the load lock, where the base pressure is higher. The temperature was measured by means of a *K*-type thermocouple in direct contact with the copper heating stage upon which the samples were cured. A control measurement, where a second thermocouple was mounted on the substrate, gave a maximum temperature difference of less than 5 °C. Spatially resolved STL images were collected while operating the STM in tunneling mode at voltages between 2 and 5 V and at constant currents up to 400 pA. This allowed the simultaneous recording of topographic and luminescence images. Measurements of wavelength-integrated luminescence intensity as well as STL spectra were carried out under field-emission (FE) conditions, where electrons are injected from the STM tip at energies in the 100-eV range. Currents were in the range 5 pA–1 nA depending on the luminescence yield.

III. RESULTS

In order to characterize the homogeneity of the samples and the emission intensity with high spatial resolution we took STM and STL images in UHV. Figure 2 shows a typical result comparing topographic and luminescence maps collected on a sample deposited on a Au/glass substrate and cured at various temperatures up to $T_c=220$ °C. The tunneling voltage was $V_T=4.6$ V and the tunneling current $i_T=340$ pA. Under these conditions no significant degradation effects of the sample are observed during the tunneling experiment (less than a factor of 2 decrease in intensity over several hours). Typically, the time required to collect an image is approximately 30 min.

The luminescence intensity pattern is neither homogeneous nor completely random with respect to the surface topography. In some regions the luminescence intensity pattern reveals a clear correlation with topographic features, whereas in others the luminescence is anticorrelated. For instance, some topographic features, e.g., hillocks, appear dark [region *A* in Fig. 2(a)], while others appear bright [region *B* in Fig. 2(a)]. The image shows wide variations of the excited luminescence intensity within domains as small as 10 nm [Figs. 2(b) and 2(c)]. Although this luminescence map is quite typical, we note that the size of the bright and dark areas varies over the sample and 100-nm-wide regions of homogeneous luminescence intensity can be found. It is also important to keep in mind that the luminescence map represents the local luminescence efficiency of the material convoluted with the local injection efficiency from the tip across the surface interface into the subsurface region. Fluctuations in luminescence efficiency of the organic material may thus appear exaggerated in the luminescence map.

Preliminary luminescence intensity vs tunneling voltage (i_L vs V_T) measurements show that the threshold for luminescence excitation varies from 1.60 to 1.8 eV depending on the tip position, suggesting variations of the electronic properties of the PPV films on a 10-nm scale.[15] In general, highly localized variations in the luminescence imply that the system is electronically, and therefore structurally, complex even at the nanometer scale and suggest that there is a potential for great improvement of the total luminescence yield.

With the present experimental configuration light intensities were insufficient to obtain luminescence spectra in tunneling mode. We therefore investigated the spectra of luminescence excited by FE. Under these conditions, luminescence arises from multiple electronic excitations created by the impact of the incident electrons, a process discussed in more detail below. In these experiments the tip-surface distance is of the order of 1 μm, which results in a spectroscopic signal averaged over an area of about 1 μm^2. The spectra are collected in the same location on the sample to within $\sim$2 mm. In several instances the tip was reposi-

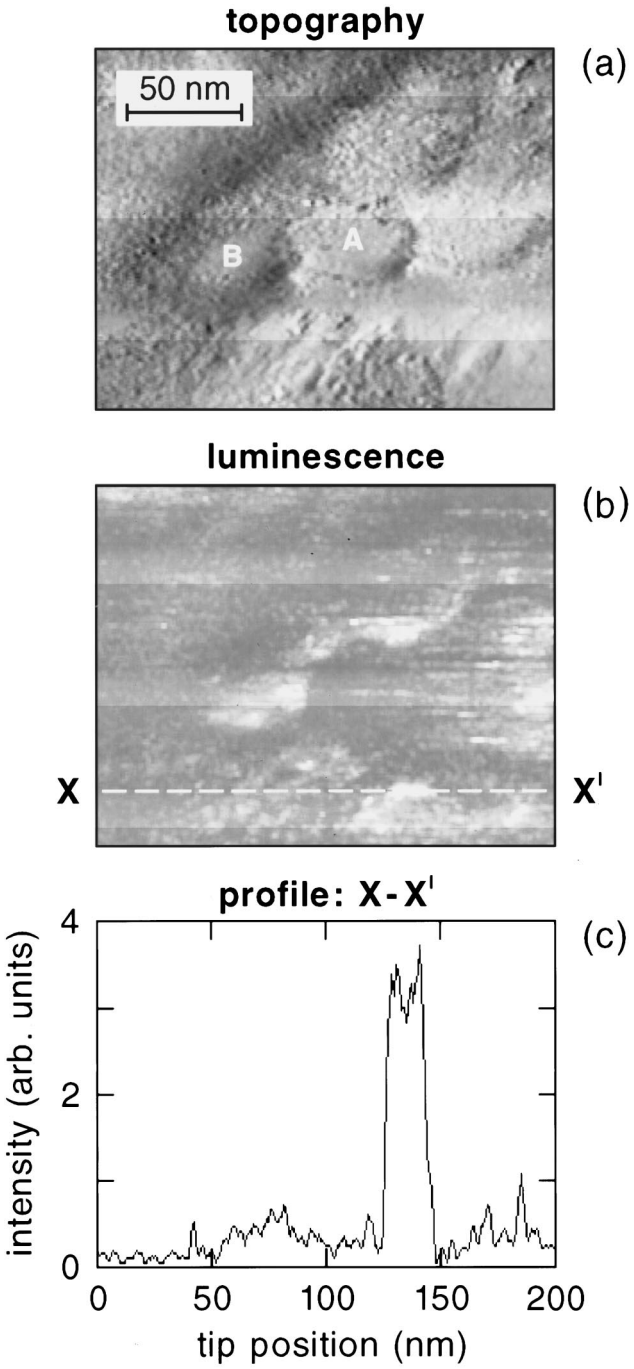

FIG. 2. Topography and luminescence maps obtained simultaneously on a PPV/Au/glass sample. The top image shows the x derivative of the topography giving the impression of illumination from the left-hand side. The surface exhibits peak-to-valley height differences of up to 7 nm. The luminescence map shows some hillocks as bright features, whereas others appear dark. Compare the luminescence of regions A and B in the topography. The profile of the luminescence intensity reveals large local fluctuations of the STL luminescence within nanometer-sized regions.

tioned by 10–30 μm to repeat a measurement and check reproducibility.

Luminescence spectra of a PPV/ITO/sapphire sample treated at progressively higher temperatures are shown in Fig. 3. As for all such spectra in this paper, the luminescence intensity is normalized to excitation power (iV). The dotted

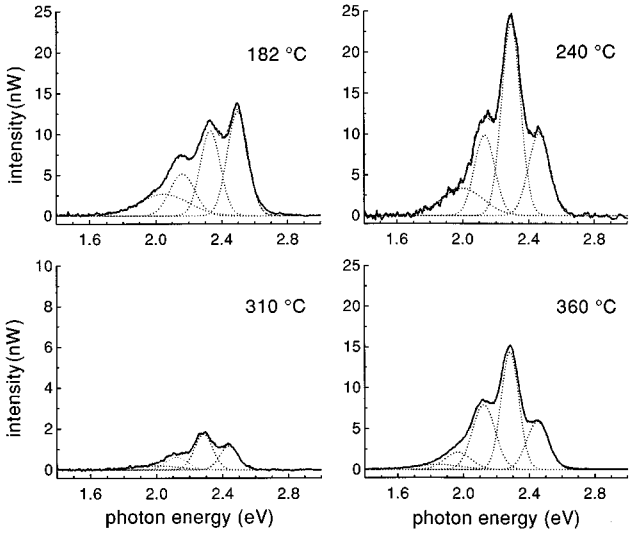

FIG. 3. Examples of STM-FE luminescence excitation spectra collected on a PPV/ITO/ sapphire sample cured *in situ* at progressively higher temperatures. Note the change in scale for the $T_c = 310\,^{\circ}\mathrm{C}$ spectrum. The measurements were taken at room temperature under UHV conditions.

lines in Fig. 3 are the result of fitting a set of multiple Gaussian functions to the data to determine the vibronic energy, linewidth, and peak area. To ensure the least possible prejudice, all of these were allowed to be free variables in the fitting procedure. No attempt was made to accommodate the different vibrational modes of the polymer chain. Normally in EL from actual OLED's as well as in PL studies of polymers, the emission arises either from a deep-lying interface or from the bulk of the organic material, which leads to enhanced self-absorption[16] and consequently to an apparent decrease of the $v = 0,0$ peak intensity. In STL the radiation is collected directly from the free surface of the sample (see Fig. 1), and because this is a surface-sensitive technique we expect an apparent enhancement of the relative intensity of the $v = 0,0$ peak. Thus this technique allows an analysis of the intrinsic vibronic spectra.

The spectra exhibit the typically observed progression of vibronic lines, which arises from Franck-Condon coupling of vibrational and electronic transitions and is often assigned to one vibrational mode, the phenyl ring stretch.[2,7,9,17,18] The data reveal a shift of the spectral weight among the various vibronic states, and this shift is not monotonic with T_c. For example, the intensity of the $v = 0,0$ relative to that of the $v = 0,1$ peak first decreases and then increases with T_c. Careful analysis indicates that the intensity ratio of these lines, $I_{0,1}(T_c)/I_{0,0}(T_c)$, reaches peak values for T_c at which the wavelength-integrated luminescence yield exhibits maxima. This behavior is observed for polymer films prepared on ITO, Au, and glass substrates and allows the quality of the organic light-emitting material to be determined by inspection of the relative vibronic peak intensities.

Figure 4 shows the peak energies of the vibronic progression as a function of T_c. The data reveal a redshift (by approximately 60 meV for the high-energy peak) for T_c in the range $180\,^{\circ}\mathrm{C} < T_c < 280\,^{\circ}\mathrm{C}$, whereas at higher temperatures the peak energies are nearly constant. The vibrational energy, i.e., the spacing between the peaks, also decreases with in-

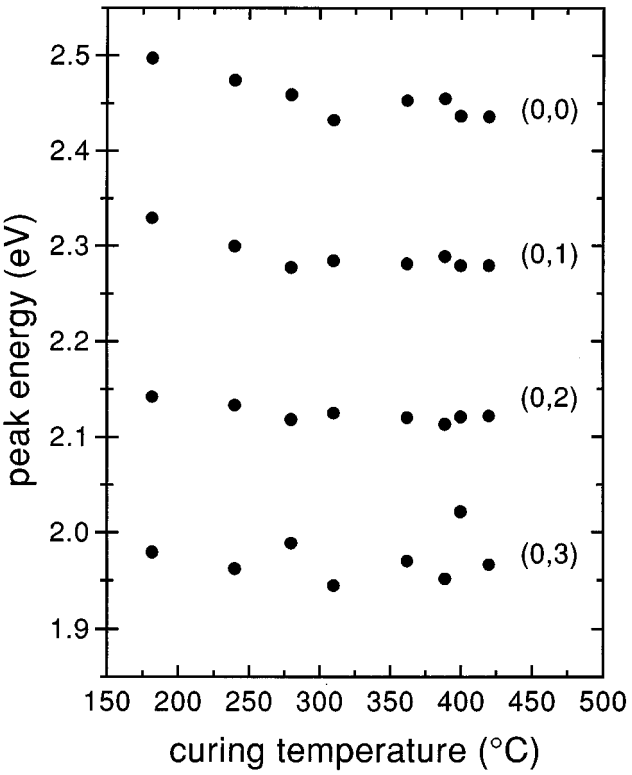

FIG. 4. Peak energy vs T_c of the vibronic progression for PPV/ITO/sapphire.

creasing temperature; the redshift is smaller for higher final-state vibrational quantum numbers v. In addition, the Gaussian linewidth, which is larger for higher v (for example 115 ± 10 meV for $v=0,0$ and 175 ± 60 meV for $v=0,3$ at $T_c=180\,^{\circ}\mathrm{C}$) tends to decrease with T_c. This reduction appears to be more pronounced for the lower energy peaks. In this case, the change in the linewidth of the $v=0,0$ peak is too small to be discerned, but is evident in other data to be discussed below. The $v=0,1$ and $v=0,2$ peaks decrease by about 20 meV, as shown in Fig. 5.

Our results are consistent with Raman and PL measurements on PPV oligomers[19] and with a comparison of the PL from PPV and *trans,trans*-distyrylbenzene.[20] These reports describe a steep redshift (greater than 200 meV) of the vibronic spectrum with increasing number (n) of phenyl rings in the range $3 \leqslant n \leqslant 6$; however, for $n \geqslant 10$ the energy of the transitions changes more slowly and differs minimally from that of PPV.[21] In addition, a decrease of vibrational energy with chain length has been reported for Raman spectra of *trans*-polyenes.[22] The redshift of the electronic transition as well as the reduction of the vibrational energy observed in our data can be similarly understood in terms of delocalization effects.

Figure 6 shows wavelength-integrated luminescence yield versus curing temperature measured on a PPV/ITO/sapphire sample. The data show a weak but reproducible local intensity maximum at $T_c \simeq 180\,^{\circ}\mathrm{C}$, whereas the highest observed intensity occurs between 240 °C and 280 °C. Thus for this sample the optimum conversion temperature is $T_{\mathrm{opc}} \simeq 260\,^{\circ}\mathrm{C}$. The temperature at which the luminescence yield abruptly begins to decrease, $T_c \simeq 280\,^{\circ}\mathrm{C}$, correlates with the region where the temperature-dependent redshift of

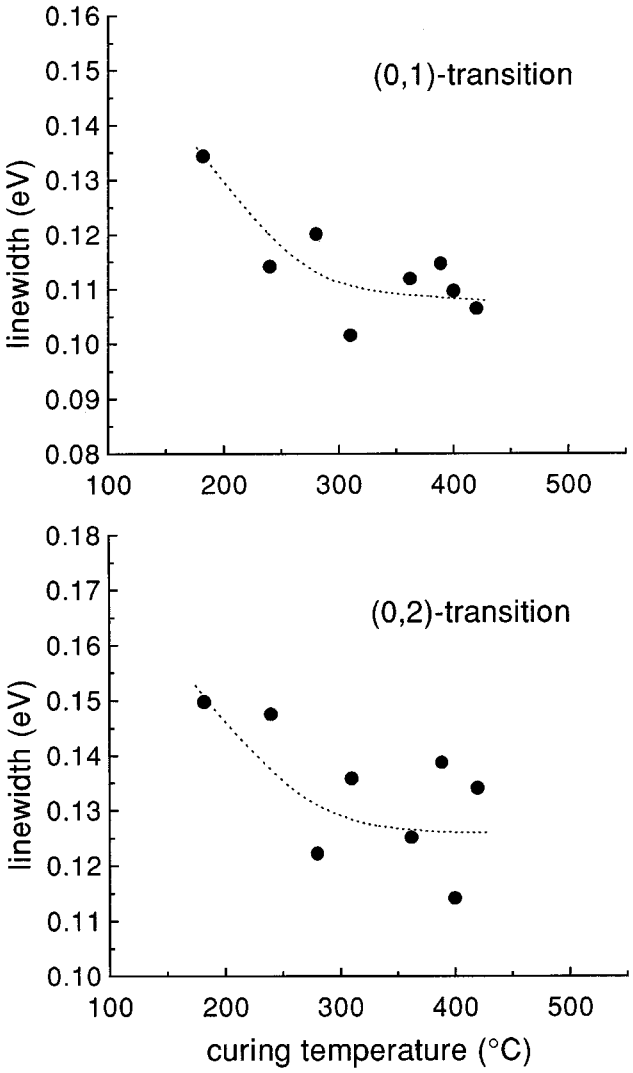

FIG. 5. Gaussian linewidth of the $v=0,1$ and $v=0,2$ vibronic peaks vs T_c for PPV/ITO/ sapphire. The dashed line is a guide to the eye.

the vibronic features becomes negligible (Fig. 5).

To elucidate the effect of chemical interactions between the substrate and polymer we have similarly analyzed samples prepared on Au/glass substrates. The substrates were made by evaporating an 80-nm-thick Au stripe a few millimeters wide onto glass, thus allowing comparative measurements of PPV in direct contact with Au or the adjacent glass substrate. The thermal treatment was essentially the same as for the ITO/sapphire substrates discussed above. A typical spectrum collected on a sample progressively cured up to $T_c=225\,^{\circ}\mathrm{C}$, measured on PPV over the Au-covered region of the sample, is shown in Fig. 7. When this particular sample was heated to temperatures as high as 490 °C, it showed no signs of decomposition under UHV conditions, i.e., we still see the typical vibronic structure, and the smooth trends in vibrational frequency and linewidth continue unbroken.

The spectra collected on the PPV-on-Au part of the sample are fairly complex and cannot be satisfactorily described by a single vibronic progression of Gaussian peaks. Spectra collected on the adjacent PPV-on-glass region, however, show features typical of, though not identical to, those

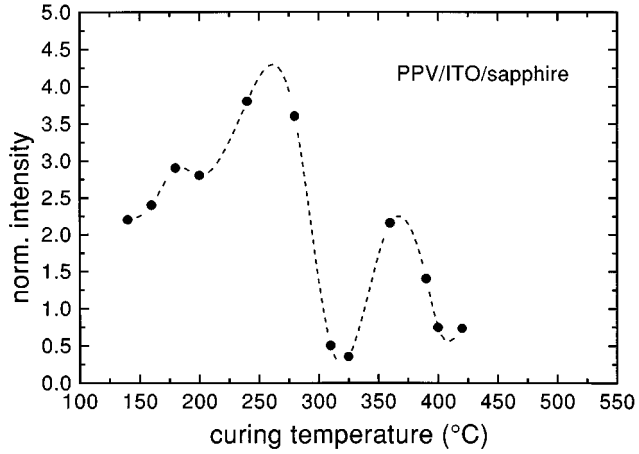

FIG. 6. Wavelength-integrated STL luminescence yield vs T_c measured on a PPV/ITO/ sapphire sample. The dashed line, a spline, serves as a guide to the eye.

found in the spectra collected from PPV-on-ITO samples (see Fig. 3). Fitting with a set of multiple Gaussians to the spectra collected on the PPV-on-Au region of the sample gave two series of lines: one characterized by very sharp features, down to 50 meV (Gaussian linewidth) for the high-energy line, and the other having linewidths a few times broader. Furthermore, the spacing between the lines is slightly greater for the latter series. Note that, owing to the complexity of the spectra, only the first few high-energy lines as well as the sharp $v=0,2$ peak can be treated as free variables. The other fitting parameters were manually fixed, i.e., for some peaks the energy spacing was forced to be approximately equidistant. As a result, the uncertainty in the linewidth and energy of the lower-energy peaks is greater than in the case of the ITO-on-sapphire substrates. Still, the fitting results for the data as a whole are consistent with two vibronic progressions. For the case of the sharp $v=0,0$ peak, the parameters are determined to high precision. Figure 8 illustrates the T_c dependence of energy and linewidth of the $v=0,0$ peak for the PPV/Au/glass sample. As was the case

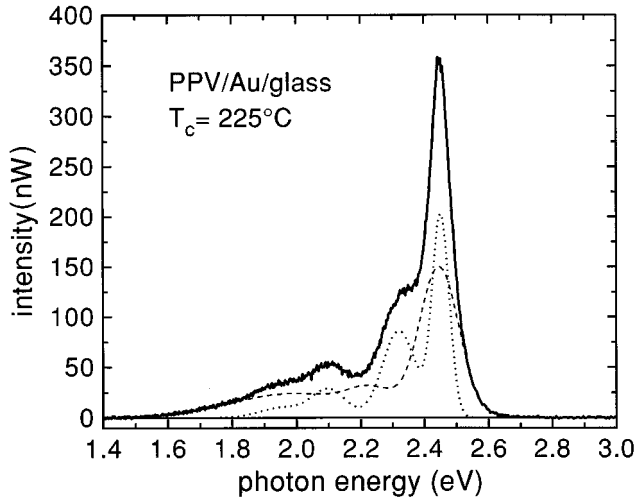

FIG. 7. Typical STL spectrum measured on a PPV/Au/glass sample after curing up to 225 °C. The dashed and dotted lines show the result of a fit to the experimental data as explained in the text.

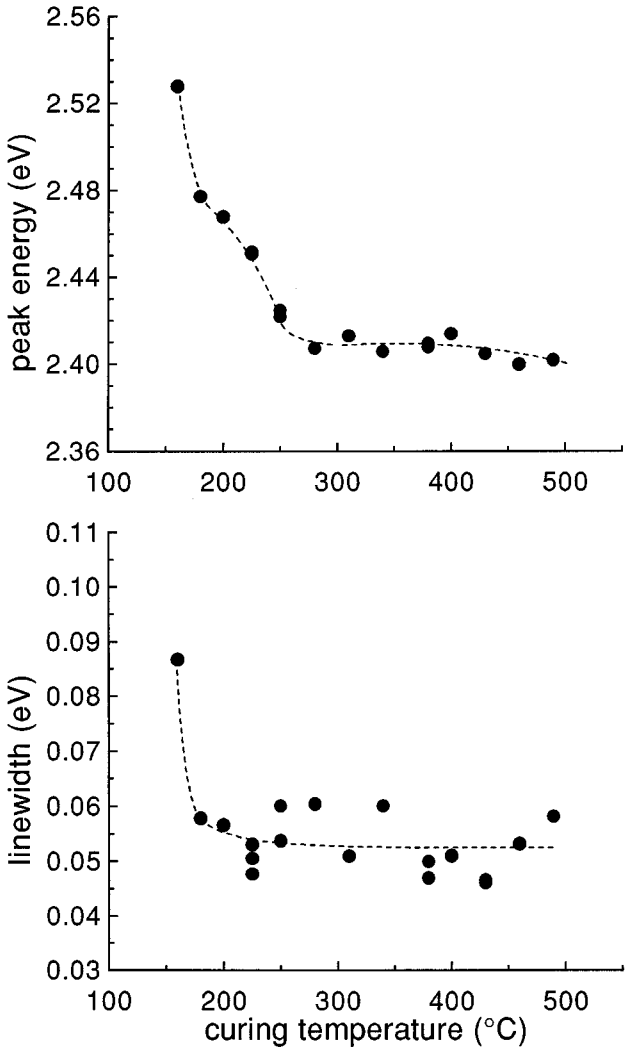

FIG. 8. Peak energy and linewidth of the sharp $v=0,0$ peak vs T_c for the PPV/Au/glass sample.

for PPV/ITO/glass, the redshift is steep in the range $160\,°\mathrm{C} \leqslant T_c \leqslant 250\,°\mathrm{C}$ and flattens out at higher curing temperatures. Note that for $T_c > 180\,°\mathrm{C}$ the linewidth of the $v=0,0$ peak decreases by about 10 meV (Fig. 8), suggesting that the homogeneity and/or ordering of the polymer continues to improve even at very high temperatures. The luminescence yield shown in Fig. 9 exhibits features in the same temperature range: a local maximum at $T_c \simeq 180\,°\mathrm{C}$ and the highest observed intensity at $T_c = 225\,°\mathrm{C}$, followed by a sharp drop. These results roughly reproduce those obtained for the ITO/sapphire substrate.

Whereas the redshift is almost independent of the underlying substrate, the luminescence yield is very sensitive to it. In general we find that luminescence from PPV cured on Au is substantially more intense than on ITO. For the specific data shown here the maximum luminescence yield from PPV on Au is more than six times higher than that from PPV on ITO substrates. Other researchers have also shown a significant impact of the substrate on the polymer; a study comparing the luminescence of PPV converted on ITO and on glass substrates reports a similar detrimental influence of ITO.[9]

We find that the details of the temperature history of a sample have a profound impact on the electro-optical prop-

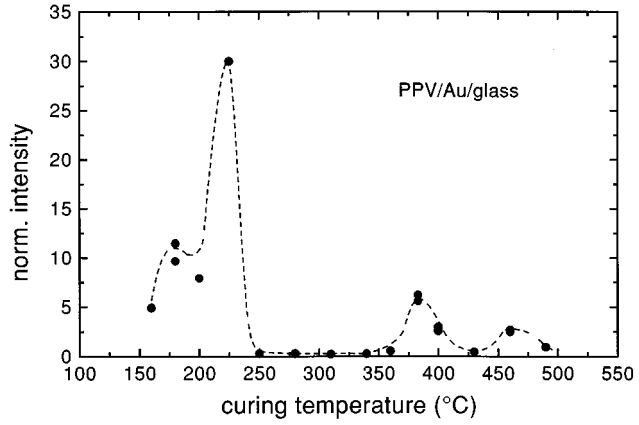

FIG. 9. Wavelength-integrated STL luminescence yield vs T_c of a PPV/Au/glass sample.

erties of the resulting polymer film. The luminescence yield as well as the relative intensity and peak energy depends strongly on the heating gradient. For example, a prepolymer film on a Au/glass substrate heated from room temperature to 225 °C in 15 min and then cured at that temperature for 2 h exhibits a higher luminescence efficiency than a sample heated to 225 °C at a rate 5 times lower. STL spectra collected on these samples are shown in Fig. 10 and should also be compared to the data in Fig. 7. As the latter sample was cycled between room temperature and progressively higher T_c it has a very different temperature history.

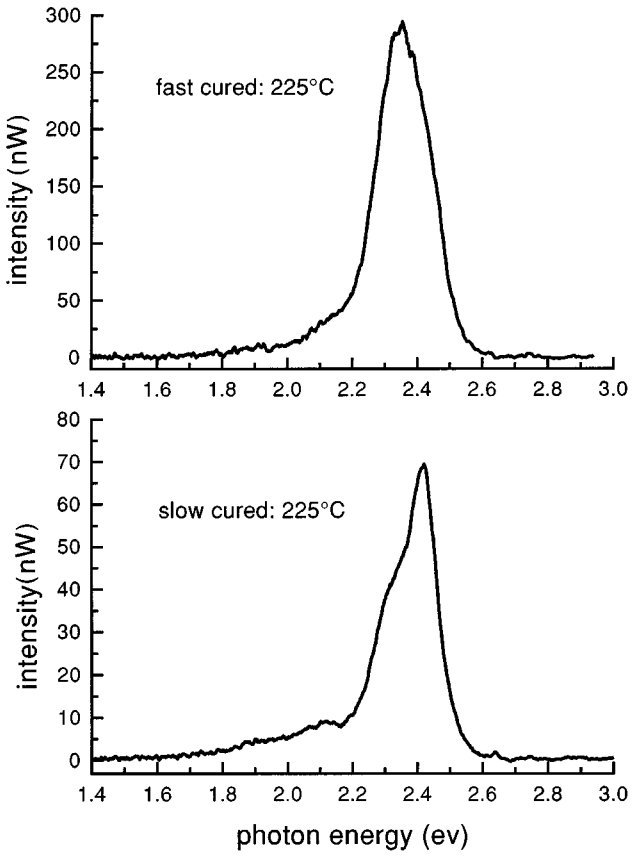

FIG. 10. STL spectra measured on a PPV/Au/glass sample after curing at different thermal gradients. Upper spectrum, collected on a sample heated from room temperature to $T_c = 225\,°C$ in 15 min; lower spectrum, collected on a sample heated to $T_c = 225\,°C$ at a rate roughly 5 times slower. The curing time is 2 h in each case.

IV. DISCUSSION

It is important to recognize that while the STL technique simulates operation of an OLED, the processes involved are actually somewhat different. The experiments carried out using the STM under FE conditions are in principle low-electron-energy cathodoluminescence measurements with submicrometer resolution. Owing to the relatively low kinetic energy of the electrons, $E_k \simeq 100$ eV, the excitations occur only within a depth of a few nanometers of the surface.[23] The probing depth is determined by this penetration length of the incident electrons as well as by the diffusion of the excitons perpendicular to the surface, which is typically in the 1–10 nm range.[25,26] The diameter of the incident electron beam is approximately equal to the tip-surface distance, which is of the order of 1 μm. Electrons impinging on the surface produce electron-hole pair excitations by inelastic scattering. In the dipole approximation these are optically allowed transitions from the filled valence states into empty excited states of the polymer. Radiative recombination can occur in all these states, but this is unlikely due to fast radiationless decay to the lowest vibrational level of the lowest π^* state. Radiative recombination from this state leads to the generation of visible light, the only radiation we monitored with our experimental apparatus. Consequently, the spectra observed while operating the STM in FE mode essentially correspond to those observed in PL and EL. The main difference from the latter techniques is that the effects of self-absorption of the emitted light are minimized.

The maximum number of excitons produced by an incident electron can be estimated as the ratio E_k/E_g, where E_g is the optical absorption energy gap. The actual number of excitons, however, is lower because higher vibronic states are also excited and, to the extent that the excess energy is dissipated, that energy does not contribute to the luminescence. Furthermore, a fraction of the incident electron beam current is elastically reflected at the polymer surface. A conservative estimate indicates that in STM-FE excitation, the internal efficiency [(total energy emitted)/(incident energy)] may be as high as 10% for PPV/Au/glass.

In the case of STL, where the tunneling voltages are low, the generation of electron-hole pairs is negligible. Additionally, at tunneling voltages close to the luminescence threshold, the energy losses associated with thermalization are minimized and hence a higher luminescence efficiency per injected electron is expected. Similar to the STM in FE mode, the probing depth is determined by the penetration depth of the injected electrons and the diffusion length of the excitons.

The observation of luminescence from the polymer in both tunneling and FE modes implies that charge neutralization occurs within the polymer. Injected electrons recombine with holes moving towards the surface under the influence of the local electric field. Note that in PPV the mobility of holes is much higher than the mobility of electrons.[24] Because of this and the diffusion length of the injected electrons[23] we

expect recombination to occur within a distance below the vacuum interface of the order of 10 nm, which is similar to what is observed in conventional PPV devices. We note, however, that due to our unique electron injection conditions the detailed charge carrier distributions may differ.

It is also interesting to consider the implications of the STL technique for degradation studies of organic materials. Regarding the tip/tunnel-barrier/PPV/substrate system as a model of an OLED, our typical experimental parameters in tunneling mode correspond to a device operating at a current density of $j \simeq 2$ kA/cm^2 and a voltage of $V \simeq 4.6$ V. Such enormous current densities, which would normally be considered unreasonable in a conventional OLED at such low voltages, are attainable because of the extremely high field at the apex of the STM tip, the radius of which is typically a few to several tens of nanometers. Scanning under these conditions, the luminescence intensity decreases by less than a factor of 2 over periods of several hours. Conventional OLED's often show a decrease of the EL intensity, which depends on the amount of charge passing through the device. In one study,[27] the dependence of the time to half brightness was found to have the form $\tau_{1/2} \propto j^{-x}$, where $1.5 \leqslant x \leqslant 1.8$. From this expression, we extrapolate that for an OLED operated at current densities $j \simeq 10$ mA/cm^2, the half-life of our PPV would exceed tens of thousands of hours even for the typically claimed Coulomb aging case, i.e., $x = 1$. It appears that PPV is intrinsically a very stable material even when subjected to high-current densities.

Owing to the intrinsically high surface sensitivity, optimum use of STL requires UHV conditions and samples prepared *in situ*. By curing prepolymer films under such conditions, we eliminated the chemical reaction of the prepolymer and of the final conjugated polymer with air, ambient contaminants, and residual gases, thus providing conditions for highly reproducible results and forming the basis for a detailed understanding and optimization of the conversion process. Residual contamination is found to be so important that not only is an improvement of the luminescence yield observed upon going from preparation under ambient, inert gas, or low-vacuum conditions (mbar range) to preparation in the 10^{-7}-mbar range, but also an additional improvement is observed when curing the samples under UHV conditions (lower 10^{-10}-mbar pressure range).

For technical applications the optimum conversion temperature and conditions at which highest luminescence is obtained are important material and device parameters. Previous reports on the curing temperature dependence of the luminescence provide an inconsistent and confusing picture: Zhang *et al.*[7] report on the conversion of a PPV prepolymer in a nitrogen flow for the temperature range $140\,^\circ\mathrm{C} < T < 300\,^\circ\mathrm{C}$. They obtain a maximum EL efficiency at $T_c \simeq 160\,^\circ\mathrm{C}$ and a strong decrease at higher temperatures. Their PL data, however, show a very different behavior: The PL efficiency remains practically constant in the range $160\,^\circ\mathrm{C} \leqslant T_c \leqslant 210\,^\circ\mathrm{C}$ and decreases by a factor of 2 for $T_c = 300\,^\circ\mathrm{C}$. In contrast, Herold *et al.*[9] find that the PL yield of PPV films decreases monotonically with increasing conversion temperature in the range $100\,^\circ\mathrm{C} < T_c < 180\,^\circ\mathrm{C}$. Papadimitrakopoulos *et al.*[8] report on PL measurements on PPV films converted under forming gas at 200 °C, 250 °C, and 300 °C, which show a monotonic decrease of the PL intensity with increasing temperature. Various explanations are invoked to explain these results, e.g., changes in the conjugation length, and carbonyl formation. We believe that the discrepancies are due to the wide range of preparation and conversion conditions used.

Our results (Figs. 6 and 9) reveal that the efficiency increases significantly in the temperature range $140\,^\circ\mathrm{C} \leqslant T_c \leqslant 225\,^\circ\mathrm{C}$. The actual rise in efficiency and the optimum conversion temperature (T_{opc}) depend on the substrate material (ITO, Au, and glass). For example, for PPV converted on Au/glass substrates an increase of the luminescence efficiency by a factor of 5 is observed and $T_{\mathrm{opc}} \simeq 225\,^\circ\mathrm{C}$ (Fig. 9), whereas for ITO/sapphire substrates the luminescence efficiency increases by a factor of only 2 and $T_{\mathrm{opc}} \simeq 260\,^\circ\mathrm{C}$ (Fig. 6). This implies an interaction between the polymer and the substrate material. For instance, In, Sn, or O from the ITO, impurities from the glass, or even Au could be diffusing into the polymer. In particular, oxygen contamination is known to give rise to carbonyl groups, which act as luminescence quenching centers.[28,29] Based on previous work,[9,29,30] we expect that in our samples In and O diffusion from ITO into the polymer give rise to a lower luminescence yield in PPV/ITO/sapphire samples compared to that of PPV/Au/glass. Such chemical interactions may also account for the fact that films cured on Au must be fit with two vibronic progressions with different energetic spacings. In this case, possible explanations include emission from at least two different phases of the polymer, some of which are more ordered than others, or a contribution of a second, strong vibrational mode in determining the transition oscillator strength. Either way, interdiffusion and/or a reaction of substrate material with the polymer could be responsible.

Heating the sample past T_{opc}, we observe a sharp drop of the luminescence yield. Preliminary thermodesorption mass spectroscopy (TMS) reveals that this transition occurs close to the temperature where the thermal desorption of hydrochloric acid and tetrahydrothiophene (THT) has been completed. Additionally, TMS results show that the desorption of THT and hydrochloric acid begin at different temperatures, the desorption of elimination products has passed its peak value for temperatures higher than about 220 °C, and the desorption of elimination products probably is not yet fully finished even at temperatures above 300 °C.[15]

The data for PPV/ITO/sapphire (Figs. 4–6) and PPV/Au/glass samples (Figs. 8 and 9) indicate that the redshift and decrease in linewidth of the vibronic features occur primarily at temperatures less than or equal to T_{opc}. The redshift of the electronic transition as well as the reduction of the vibrational energy observed can be understood in terms of delocalization effects. This may include not only an increase of conjugation length but also intra- and interchain coupling and ordering, which are also directly reflected by the width of the spectral features. Furthermore, the dependence of the linewidth on the vibrational quantum number v can be understood by considering that variations of the vibrational energy associated with the amount of disorder in the polymer are weaker for the transitions involving levels closer to the potential minimum.

Taken together, the phenomena that we observe up to T_{opc} are consistent with an increase in (i) the chemical homogeneity and (ii) intra- and interchain order of the polymer.

One would expect that the concomitant increase of the effective conjugation length would lead to an enhancement of the exciton mobility. This in turn should give rise to enhanced quenching at nonradiative defects and thus would cause a decrease in luminescence efficiency. Our results indicate that this is actually not the case, at least in the temperature range below the optimum curing temperature. We conclude that for our samples treated under UHV conditions, in contrast to less clean environments, increasing T_c leads to an increase of the conjugation length *and* to the elimination of intrinsic quenching impurities and imperfections without suffering the consequences of ambient-induced defect production, e.g., carbonyl formation.

Above T_{opc}, the trade-off between removal of quenching sites and enhanced exciton mobility appears to become suddenly unfavorable. We can speculate that at high temperatures either new defects are being generated or a new mechanism for significantly enhanced exciton mobility has become available. The latter might result from increased long-range order of the polymer film. In any case, the continued, albeit smaller, oscillations in overall intensity and spectral features with increasing temperature indicate that complex processes are involved. Work continues toward elucidating this high-curing-temperature behavior.

We also find that the thermal treatment influences the Franck-Condon intensity distribution of vibronic transitions. For example, the spectra for PPV/ITO/sapphire (Fig. 3) show that in the range $T_c = 180\,^{\circ}\mathrm{C}$–$240\,^{\circ}\mathrm{C}$, where the yield increases with temperature, the intensity maximum shifts from the $v = 0{,}0$ towards the $v = 0{,}1$ transition. To interpret this result we recall that the luminescence yield is determined by the probability amplitude for vibronic transitions

$$T_{um,ln} = T_{ul}\langle \chi_{um} | \chi_{ln} \rangle, \tag{1}$$

where T_{ul} is the purely electronic transition amplitude evaluated at the equilibrium position of the nuclei. The χ terms are the vibrational state wave functions for the upper (u) and lower (l) potentials. The absolute square of $\langle \chi_{um} | \chi_{ln} \rangle$ is the Franck-Condon factor, which in a simplified picture[31] gives an intensity of the $v = 0,m$ vibrational transition proportional to

$$I_{0,m} = \left(\frac{\langle \tilde{\nu}_{lm,u0} \rangle}{\langle \tilde{\nu}_{l0,u0} \rangle} \right) \frac{Z^m}{m!} e^{-Z}, \tag{2}$$

where $\langle \tilde{\nu}_{lm,un} \rangle$ is the mean wave number of the $v = n,m$ vibronic transition and

$$Z = \frac{1}{2} k (\Delta Q)^2 / \hbar\omega. \tag{3}$$

Here k and $\hbar\omega$ are the force constant and the vibrational energy and ΔQ is the displacement of the equilibrium position of the upper and lower electronic potentials in the configuration coordinate Q. From Eqs. (2) and (3) we deduce that the observed intensity shift from the $v = 0{,}0$ towards the $v = 0{,}1$ transition implies an increase of ΔQ (Ref. 32) with curing temperature, i.e., with increasing effective conjugation length, in the range $T_c \leqslant T_{\mathrm{opc}}$. Furthermore, the sudden drop of luminescence, which occurs between T_{opc} and $T_c = 310\,^{\circ}\mathrm{C}$ (Fig. 6) is accompanied by a sharp reduction of the relative intensity of the $v = 0{,}1$ vibronic peak (Fig. 3). The data indicate that the relative intensity of the $v = 0{,}1$ transition is maximal for $T_c \simeq T_{\mathrm{opc}}$. This demonstrates the influence of the curing conditions on the interplay between the configurational changes (ΔQ) of the polymer upon optical excitation, the vibrational transitions, and the luminescence yield, the optimum tuning of which is identifiable through a particular and characteristic Franck-Condon intensity distribution of the luminescence spectrum.

For $T_c \simeq 360\,^{\circ}\mathrm{C}$, where a local luminescence maximum occurs (Fig. 6), we find that the relative intensity of the $v = 0{,}1$ transition also shows a local maximum. The same phenomenological behavior is observed on PPV/Au/glass and PPV/glass samples: an intensity shift from the $v = 0{,}0$ towards the $v = 0{,}1$ line for $T_c \leqslant T_{\mathrm{opc}}$, and for higher values of T_c, oscillations of the relative intensity of the $v = 0{,}1$ transition in phase with local luminescence maxima. Surprisingly, the latter oscillations occur in a curing temperature range where the redshift of the vibronic lines indicates that the effective conjugation length continues to increase, though only slightly, with temperature. This observation suggests that the luminescence efficiency is strongly influenced by subtle geometrical details of the polymer, e.g., bond-length changes, intra- and interchain order, and formation of defects and crystallites. These processes can in turn be influenced by chemical interaction with the underlying substrate (*vide supra*), the extent of which is likely to increase at higher temperatures. An indication of chemical effects on the spectral intensity distribution has been reported for metal/PPV/ITO devices,[33] where the precursor was cured in low vacuum at $T_c = 300\,^{\circ}\mathrm{C}$. That work shows that the intensity distribution of the vibronic peaks depends on the cathode metal (Ca, Mg, In, and Al), but no mention is made of the effect of the cathode material on luminescence efficiency.

Finally, given the apparent influence of homogeneity and chemical composition, the strong changes of the spectral intensity distribution observed for various temperature gradients (Figs. 7 and 10) is hardly surprising. One naturally expects a competition between chemical reactions, mass transport, and ordering processes for the condensed-phase conversion process studied here. Depending on which of these is rate limiting, the properties of the resulting polymer can vary widely and several factors in addition to the temperature gradient could influence the balance between rates. For example, curing in inert atmosphere is expected to inhibit desorption of elimination products compared to curing in vacuum. Such effects explain the diversity of results on a material that is nominally always the same, ''PPV.''

V. CONCLUSION

In order to fabricate polymer-based OLED's with the highest possible performance, it is of great utility to understand which factors in polymer film formation determine luminescence efficiency and how these factors can be controlled. This is particularly true for a process as complicated as the thermal conversion of poly(p-phenylene-ethylene-tetrahydrothiophenium chloride) into PPV. It is towards this end that we have investigated this prepolymer curing process over the wide temperature range $100\,^{\circ}\mathrm{C}$–$490\,^{\circ}\mathrm{C}$. By combining highly localized, surface-specific

spectroscopic STL measurements with curing in an UHV environment, we are uniquely able to probe prepolymer conversion under well-defined conditions. The results obtained for PPV have manifold implications for the fabrication of polymer-based OLED's in general.

We find, in contrast to previous reports, that the luminescence efficiency increases by a factor of 2–5 as the curing temperature is increased from 140 °C to the optimum temperature of T_{opc}, where T_{opc} is between 225 °C and 260 °C. In this temperature range, the redshift of the vibronic transitions observed in EL, the decrease in linewidth, and the decrease in vibrational spacing all point to an increase in order and effective conjugation length of the polymer with T_c, in other words, to the formation of a more ''perfect'' polymer film. Under our conditions, therefore, it seems that a positive trade-off can be achieved between removal of luminescence quenching sites and enhancement of exciton mobility. We believe this is a direct consequence of suppressing deleterious chemical side reactions, such as reactions between atmospheric gases and the polymer, by curing in UHV. Beyond T_{opc}, though, it appears that the favorable balance is suddenly lost, either because defects are now generated or because additional exciton diffusion pathways are opened, both of which could create new quenching mechanisms. Similar trade-offs are likely to be important in other polymer systems.

The value of T_{opc}, the total luminescence yield, and the details of the spectra for a given sample depend on the underlying substrate and the heating gradient. These dependences are a reflection of various chemical reactions and their relative rates, which suggests that other factors, which we have only begun to explore, are also quite important. These include thickness of the polymer film and variations in initial composition, such as purity and solvent content of the prepolymer. The consequence for OLED operation is that less surface and bulk contamination of the polymer should lead to more efficient charge carrier injection, reduced luminescence quenching, and overall improved luminescence efficiency.

We have also discovered a surprising correlation between luminescence yield and the Franck-Condon intensity distribution of the vibronic transitions in PPV. The relative intensities of the $v=0,0$ and $v=0,1$ transitions oscillate in phase with the luminescence intensity as a function of temperature. Near T_{opc}, where the wavelength-integrated luminescence efficiency is maximum, the relative intensity of the $v=0,1$ transition is also maximum and this peak dominates the vibronic distribution. This suggests an intriguing means of monitoring polymer film quality.

Perhaps the most important observations, however, come from the STL imaging experiments under tunneling conditions. The extreme variation in emission intensity on the nanometer scale clearly indicates that there is considerable room for improvement of average film luminance. But it is important to keep in mind that local variations of the injection efficiency play a role. Moreover, the relatively slow degradation of our polymer films for both tunneling and FE measurements, as well as the fact that films treated at temperatures approaching 500 °C still yield substantial luminescence, illustrates the intrinsically high stability of PPV. The slow degradation of the polymer films observed under tunneling conditions, where the current densities are enormous, indicate that times to half brightness in actual OLED's could easily exceed 10 000 h.

ACKNOWLEDGMENTS

P. S. thanks the IBM Zurich Research Laboratory for hosting his visit. The authors thank R. Brütting (Universität Bayreuth) for synthesizing the PPV prepolymer. Many thanks to E. Delamarche, H. Vestweber, W. Andreoni, and A. Curioni for enlightening discussions. Thanks also to G. Sasso for the preparation of the substrates, to F. K. Reinhart for lending very useful equipment.

*Author to whom correspondence should be addressed. Electronic address: alv@zurich.ibm.com

[1] C. W. Tang, Inf. Dis. **12**, 16 (1996); N. C. Greenham and R. H. Friend, Solid State Phys. **49**, 1 (1995); J. R. Sheats, H. Antoniadis, M. Hueschen, W. Leonard, J. Miller, R. Moon, D. Roitman, and A. Stocking, Science **273**, 884 (1996).

[2] J. H. Burroughes, D. D. C. Bradley, A. R. Brown, R. N. Marks, K. Mackay, R. H. Friend, P. L. Burns, and A. B. Holmes, Nature (London) **347**, 539 (1990).

[3] D. Braun and A. J. Heeger, Appl. Phys. Lett. **58**, 1982 (1991).

[4] N. C. Greenham, S. C. Moratli, D. D. C. Bradley, R. H. Friend, and A. B. Holmes, Nature (London) **365**, 628 (1993).

[5] R. H. Friend, G. J. Denton, J. J. M. Halls, N. T. Harrison, A. B. Holmes, A. Kohler, A. Lux, S. C. Moratti, K. Pichler, N. Tessler, and K. Towns, Synth. Met. **84,** 463 (1997).

[6] D. D. C. Bradley, J. Phys. D **20**, 1389 (1987).

[7] C. Zhang, D. Braun, and D. Heeger, J. Appl. Phys. **73**, 5177 (1993).

[8] F. Papadimitrakopoulos, K. Konstadinidis, T. M. Miller, R. Opila, E. A. Chandross, and M. E. Galvin, Chem. Mater. **6**, 1563 (1994).

[9] M. Herold, J. Gmeiner, W. Rieß, and M. Schwoerer, Synth. Met. **76**, 109 (1996).

[10] J. K. Gimzewski, B. Reihl, J. H. Coombs, and R. R. Schlittler, Z. Phys. B **72**, 497 (1988); J. H. Coombs, J. K. Gimzewski, B. Reihl, and J. K. Sass, J. Microsc. **152**, 325 (1988).

[11] S. F. Alvarado, Ph. Renaud, D. L. Abraham, Ch. Schönenberger, D. J. Arent, and H. P. Meier, J. Vac. Sci. Technol. B **9**, 409 (1991).

[12] Ph. Renaud and S. F. Alvarado, Phys. Rev. B **44**, 6340 (1991).

[13] M. Pfister, M. B. Johnson, S. F. Alvarado, H. W. M. Salemink, U. Marti, D. Martin, F. Morier-Genoud, and F. K. Reinhart, Appl. Phys. Lett. **65**, 1168 (1994); M. Pfister, Ph.D. thesis, Ecole Polytechnique Fédérale de Lausanne, 1995.

[14] M. Herold, J. Gmeiner, and M. Schwoerer, Acta Polym. **45**, 392 (1992); J. Gmeimer, S. Karg, M. Meier, W. Rieß, P. Strohriegl, and M. Schwoerer, *ibid.* **44**, 201 (1993).

[15] S. F. Alvarado, W. Rieß, and P. F. Seidler (unpublished).

[16] D. D. C. Bradley, Synth. Met. **54**, 401 (1993).

[17] F. Cacialli, X.-C. Li, R. H. Friend, S. C. Moratti, and A. B. Holmes, Synth. Met. **75**, 161 (1995).

[18] D. Halliday, P. L. Burn, D. D. C. Bradley, R. H. Friend, O. M. Gelsen, A. B. Holmes, A. K. Josef, H. F. Martens, and K. Pichler, Adv. Mater. **5**, 40 (1993).

[19] S. C. Graham, D. D. C. Bradley, R. H. Friend, and C. Spangler,

Synth. Met. **41-42**, 1277 (1991).
[20] N. F. Colaneri, D. D. C. Bradley, R. H. Friend, P. L. Burn, A. B. Holmes, and C. W. Spangler, Phys. Rev. B **42**, 11 670 (1990).
[21] H. S. Woo, O. Lhost, S. C. Graham, D. D. C. Bradley, R. H. Friend, C. Quattrocchi, J. L. Brédas, R. Schenk, and K. Müllen, Synth. Met. **59**, 13 (1994).
[22] C. Castiglioni, M. Del Zoppo, and G. Zerbi, J. Raman Spectrosc. **24**, 485 (1993).
[23] M. P. Seah and W. A. Dench, Surf. Interface Anal. **1**, 2 (1979).
[24] H. Meyer, D. Haarer, H. Naarmann, and H. H. Hörhold, Phys. Rev. B **52**, 2587 (1995).
[25] C. Adachi, T. Tsutsui, and S. Saito, Optoelectron., Devices Technol. **6**, 25 (1991).
[26] C. W. Tang, S. A. VanSlyke, and C. H. Chen, J. Appl. Phys. **65**, 3610 (1989).
[27] Y. Sato, S. Ichinosawa, and H. Kanai, in *Inorganic and Organic Electroluminescence*, edited by R. H. Mauch and H.-L. Gumlich (Wissenschaft und Technik, Berlin, 1996).
[28] M. Yan, L. J. Rothberg, F. Papadimitrakopoulos, M. Galvin, and T. M. Miller, Phys. Rev. Lett. **73**, 744 (1994).
[29] J. C. Scott, J. H. Kaufman, P. J. Brock, R. DiPietro, J. Salem, and J. A. Goitia, J. Appl. Phys. **79**, 2745 (1996).
[30] W. Rieß, Habilitation, University of Bayreuth, Germany, 1996.
[31] M. Pope and C. E. Swenberg, *Electronic Processes in Organic Crystals* (Oxford University Press, Oxford, 1982).
[32] A rough estimate indicates that the reduction of the vibrational energy with T_c is too small to account for the observed intensity shift.
[33] J. Peng, B.-Y. Yu, C.-H. Pyun, C.-H. Kim, K.-Y. Kim, and J.-I. Jin, Jpn. J. Appl. Phys. 2, Lett. **35**, L317 (1996).